THE JOURNAL OF PHYSICAL CHEMISTRY C

Article

pubs.acs.org/JPCC

Debye Length Dependence of the Anomalous Dynamics of Ionic Double Layers in a Parallel Plate Capacitor

R. J. Kortschot, A. P. Philipse, and B. H. Erné*

Van 't Hoff Laboratory for Physical and Colloid Chemistry, Debye Institute for Nanomaterials Science, Utrecht University, Padualaan 8, 3584 CH Utrecht, The Netherlands

ABSTRACT: The electrical impedance spectrum of simple ionic solutions is measured in a parallel plate capacitor at small applied ac voltage. The influence of the ionic strength is investigated using several electrolytes at different concentrations in solvents of different dielectric constants. The electric double layers that appear at the electrodes at low frequencies are not perfectly capacitive. At moderate ionic strength, ion transport agrees with a model based on the Poisson−Nernst−Planck (PNP) equations. At low ionic strength, double layer dynamics deviate from the PNP model, and the deviation is well described by an empirical function with only one fit parameter. This deviation from the PNP equations increases systematically with increasing Debye length, possibly caused by the long-range Coulomb interaction.

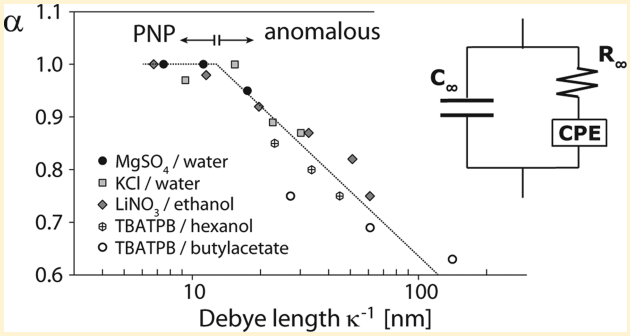

1. INTRODUCTION

The accumulation of charged species near an electrode, so-called electrode polarization, occurs in and complicates dielectric spectroscopy measurements of, for instance, biological materials,[1] solids,[2] and colloidal dispersions.[3] Additionally, electrode polarization is also a fundamental process for applications such as fuel cells,[4] supercapacitors,[4] and electrophoretic displays,[5] and it can be used for the manipulation and characterization of red blood cells.[6]

Measurements of electrode polarization often exhibit "capacitance dispersion"; that is, the double layer capacitance appears to be frequency dependent.[7−10] A satisfying physical model to describe this effect, however, is still lacking. Experimental data of relaxation behavior are often described by (semi)empirical functions,[11,12] and capacitance dispersion is usually modeled by a constant phase element (CPE). This equivalent element in an electric circuit has an impedance $Z^{-1} = A_\alpha(i\omega)^\alpha$, with $0 < \alpha \leq 1$ and A_α a constant with units Ω^{-1} s^α. The presence of fractal units when $\alpha < 1$ complicates the physical interpretation of a CPE.[13] Whether the term "double layer capacitance" then still applies to a CPE response has been debated.[14−19]

Our objective here is to enhance the physical and quantitative understanding of the frequency dependence of the double layer capacitance. Our approach is to perform a systematic study of electrode polarization of simple ionic solutions with several electrolytes of known diffusion coefficients in solvents with different dielectric constants. The electrical impedance is measured in the limit of a small applied voltage. In particular, we examine how capacitance dispersion is affected by the ionic strength, and we focus on electrode polarization in the frequency range above the characteristic frequency of double layer relaxation. Our data are compared with a simple model that takes into account diffusion and drift[20] and an empirical extension of this model with a specific form of a CPE.[21]

This paper starts with a theoretical discussion of electrode polarization in section 2 and a description of our experimental methods in section 3. Then data are presented and fitted in section 4. Finally, a general discussion is made in section 5 and conclusions are drawn in section 6.

2. THEORY

As a simple model for electrode polarization, we consider the response of a symmetric electrolyte in an isotropic solvent, confined between two blocking electrodes of a parallel plate capacitor, to which a small ac voltage is applied. Ionic transport in the direction perpendicular to the electrodes (z-axis) as a function of time t is assumed to occur according to the Poisson−Nernst−Planck (PNP) model, which consists of the following three equations. First, the fluxes $J_\pm$ of positive or negative ions with concentrations $n_\pm(z, t)$ are due to diffusion in a concentration gradient $\partial n_\pm(z,t)/\partial z$ and drift in a gradient of the electrostatic potential $\partial V(z, t)/\partial z$:

$$J_\pm(z,t) = -D\left(\frac{\partial n_\pm(z,t)}{\partial z} \pm \frac{q}{kT} n_\pm(z,t)\frac{\partial V(z,t)}{\partial z}\right) \quad (1)$$

Second, the gradient in the electric field is determined by the Poisson equation:

$$\frac{\partial^2 V(z,t)}{\partial z^2} = -\frac{q}{\epsilon_0 \epsilon_s}(n_+(z,t) - n_-(z,t)) \quad (2)$$

Received: March 13, 2014
Revised: April 22, 2014
Published: May 9, 2014

   dx.doi.org/10.1021/jp5025476 | J. Phys. Chem. C 2014, 118, 11584−11592

Third, conservation of particles is formulated in the equation of continuity:

$$\frac{\partial n_{\pm}(z,t)}{\partial t} = -\frac{\partial J_{\pm}(z,t)}{\partial z} \tag{3}$$

In these equations, k is the Boltzmann constant, T is the temperature, q is the absolute ion charge, D is the diffusion coefficient, ϵ_0 is the vacuum permittivity, and ϵ_s is the dielectric constant of the solvent.

The response of the electric cell, as a result of the PNP equations (eqs 1−3), can be expressed as the impedance $Z(\omega)$, or alternatively as a complex capacity $C(\omega)$ or a complex relative permittivity $\epsilon(\omega)$:

$$Z(\omega) = \frac{1}{i\omega C(\omega)} = \frac{d}{i\omega A\epsilon_0\epsilon(\omega)} \tag{4}$$

with $i = (-1)^{1/2}$, $\omega = 2\pi f$ the angular frequency, A the surface area of the electrodes, and d the distance between the electrodes. The frequency response of the PNP model was first derived, in a more general form, by Macdonald,[20] through linearization of the ion concentrations and assuming blocking electrodes and conservation of the number of ions (derivation in refs 20 and 22):

$$\epsilon(\omega) \equiv \epsilon'(\omega) - i\epsilon''(\omega) = \frac{\frac{1}{2}d\epsilon_s\lambda^2}{(\kappa^2/\lambda)\tanh(\lambda d/2) + i(\omega d/2D)} \tag{5}$$

with $\epsilon'(\omega)$ and $\epsilon''(\omega)$, respectively, the real and imaginary parts of $\epsilon(\omega)$ and κ^{-1} the Debye length, for a symmetric electrolyte:

$$\kappa^{-1} = \sqrt{\epsilon_0\epsilon_s kT/(2nq^2)} \tag{6}$$

and with $2n$ the average free ion number density and $\lambda = (\kappa^2 + i\omega/D)^{1/2}$. The frequency dependent conductivity is defined as $\sigma(\omega) = \omega\epsilon_0\epsilon''(\omega)$. In the limit of high frequency, the conductivity converges to a constant value σ_∞. For a symmetric electrolyte, the conductivity $\sigma_\infty = 2nq\mu_i$ with μ_i the ionic mobility can conveniently be written as $\sigma_\infty = \epsilon_0\epsilon_s D\kappa^2$, where the Einstein relation $D = \mu_i kT/q$ was used. Equation 5 is plotted in terms of $\epsilon'(\omega)/\epsilon_\infty$ and $\sigma(\omega)/\sigma_\infty$ as a function of frequency in Figure 1

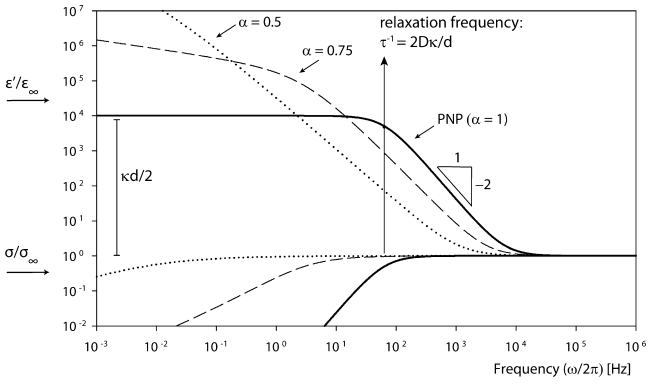

Figure 1. Theoretical response of a monovalent electrolyte with diffusion coefficient $D = 1 \times 10^{-10}$ m^2 s^{-1}, Debye length $\kappa^{-1} = 5$ nm, and electrode spacing $d = 100$ μm according to the PNP model (eq 7) (solid line), or that of the empirical model (eq 10) with $\alpha = 0.75$ (dashed line), or $\alpha = 0.5$ (dotted line).

(solid lines), corresponding to the equivalent circuit in Figure 2a. In this representation, the absence of electrode polarization at high frequencies is characterized by $\epsilon'(\omega)/\epsilon_\infty = \sigma(\omega)/\sigma_\infty = 1$;

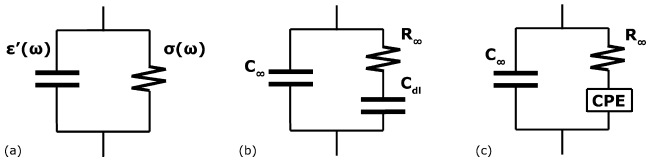

Figure 2. Schematic overview of equivalent circuits of (a) the complex permittivity in terms of frequency-dependent parameters $\epsilon'(\omega)$ and $\sigma(\omega)$, (b) the PNP model (eq 7), and (c) the empirical model (eq 10).

hence the permittivity is equal to that of the solvent, $\epsilon'_\infty = \epsilon_s$, and the conductivity is σ_∞. In the limit of low frequency, ions of one type accumulate at one electrode. The flux of ions due to diffusion and the flux due to drift cancel, and an equilibrium ionic double layer is present at each electrode, which strongly enhances the permittivity: $\epsilon'_{\omega\to 0}/\epsilon_s = \kappa d/2$.

Above the double layer relaxation frequency, electrode polarization of order 1 or more ($\epsilon'/\epsilon_\infty - 1 \geq 1$) occurs with a ω^{-2} frequency dependence,[23] as indicated in Figure 1 by the slope of −2. In the limit of high frequency, a very small contribution to the permittivity ($\epsilon'/\epsilon_\infty - 1 \ll 1$) is present with a $\omega^{-3/2}$ frequency dependence,[23] though it is not visible in Figure 1. Experimental observations of strong electrode polarization with a $\omega^{-3/2}$ frequency dependence have on occasion been ascribed to the PNP model, but this is incorrect, as was recently commented on by Hollingsworth.[24]

The exact solution (eq 5) is, for $\kappa^{-1} \ll d$ (which is valid for our data), to a very good approximation equal to the Debye relaxation function:[25−28]

$$\epsilon(\omega) = \epsilon_s + \frac{\Delta\epsilon}{1 + i\omega\tau} \tag{7}$$

with $\Delta\epsilon = \epsilon_s\kappa d/2$ and the double layer relaxation time[25,26] $\tau = d/(2D\kappa)$. The response of this Debye function can also be produced by the equivalent electrical circuit shown in Figure 2b. In this circuit, $C_{dl} = A\epsilon_0\epsilon_s\kappa/2$ accounts for the double layers at both electrodes, $R_\infty = d/(A\sigma_\infty)$ accounts for the electrolyte conductivity, and $C_\infty = A\epsilon_0\epsilon_s/d$ accounts for the dielectric response of the solvent.

One empirical model in particular,[21] an extension of the PNP model just presented, appears successful in describing our experimental data. It has been found useful before to fit electrode polarization data,[29] and here, it is tested for a wider set of dielectric constants and ionic strengths. This model is, to a very good approximation, equal to an equivalent circuit (Figure 2c) of electrode polarization in which the double layer capacitance is replaced by a CPE with an impedance of the specific form

$$Z_{CPE}^{-1}(\omega) = \frac{C_{dl}}{\tau_\infty}(i\omega\tau_\infty)^\alpha \tag{8}$$

with $0 < \alpha \leq 1$ and the Maxwell−Wagner relaxation time $\tau_\infty = R_\infty C_\infty = \epsilon_0\epsilon_s/\sigma_\infty$. The total impedance of the equivalent circuit (Figure 2c) is then given by

$$Z(\omega) = \frac{Z_{CPE} + R_\infty}{1 + i\omega C_\infty(Z_{CPE} + R_\infty)} \tag{9}$$

and the corresponding complex permittivity, using eq 4, by

$$\epsilon(\omega) = \epsilon_s + \frac{\Delta\epsilon}{(i\omega\tau_\infty)^{1-\alpha} + i\omega\tau} \tag{10}$$

In the case of $\alpha = 1$, the CPE reduces to a double layer capacitance, and the equivalent circuit reduces to that of the

dx.doi.org/10.1021/jp5025476 | J. Phys. Chem. C 2014, 118, 11584−11592

Debye function (eq 7). The responses for $\alpha = 0.5$ and $\alpha = 0.75$ are plotted in Figure 1. Decreasing the CPE exponent α leads to an apparently slower buildup of the double layer; above the double layer relaxation frequency τ^{-1}, ϵ' shows an $\omega^{-1-\alpha}$ frequency dependence. At even lower frequencies ϵ' does not level off to a constant value but remains frequency dependent with an $\omega^{\alpha-1}$ frequency dependence.

3. EXPERIMENTAL METHODS

Ionic solutions were prepared from weighed amounts of KCl (99+ %, Acros), $MgSO_4 \cdot 7H_2O$ (>99.5%, Fluka), $LiNO_3$ (99+%, Merck), tertbutylammonium tertphenylborate (TBATPB, ≥99.0%, Fluka), demineralized water (Millipore), ethanol (p.a., Merck), 1-hexanol (98%, Sigma-Aldrich), and butyl acetate (99+ %, Janssen Chimica). Ethanol was deionized with resin prior to use (BioRad, AG 501-X8 20-50 mesh (D)). TBATPB was chosen as electrolyte in apolar solvents, because the relatively large ions dissociate more easily than smaller ions. Dissolving TBATPB was accelerated by sonication for 1 h. All solutions were prepared at least 24 h before performing the measurements.

Two capacitors were used for the measurements, which were calibrated with solvents of known dielectric constant. One capacitor has a gold and an ITO electrode, glued together on the edges with adhesive (Araldite, AW2101/HW2951), through which 75 μm glass beads (Sigma-Aldrich) are mixed. This capacitor has a cell constant K_c = 28.70 pF ($C_\infty = K_c\epsilon_s$) and a surface area A = 3.066 cm^2, from which we calculate the electrode spacing d = 94.6 μm. The other capacitor has two gold electrodes, separated by a Teflon sheet. This capacitor has a cell constant K_c = 24.03 pF and a surface area A = 14.95 cm^2, from which we calculate the electrode spacing d = 551 μm.

Dielectric spectra were recorded with a differential complex permittivity setup.[30] The setup was not used in its differential mode, but the voltage was measured over a measurement resistor in series with the capacitor directly. Measurements were performed upon applying a voltage of 25 mV in the frequency range of 10^{-1} to 10^6 Hz at a temperature of either 293 or 295 K. It was verified that the response was independent of the applied voltage; deviations were only observed at a voltage of ≥1 V, and in that case only at the lowest frequencies (<1 Hz). For each measurement, the capacitor was filled with fluid and was allowed to equilibrate. Dielectric spectra did not change over time and were reproducible upon refilling with the same sample.

4. RESULTS

The complex permittivity was measured for various electrolytes with known diffusion coefficients in solvents of different dielectric constants, each at different concentrations: KCl in water (Figure 3a), $MgSO_4$ in water (Figure 3b), tertbutylammonium tertphenylborate (TBATPB or $(Bu_4N)^+(Ph_4B)^-$) in butyl acetate (Figure 4a), TBATPB in hexanol (Figure 4b), and $LiNO_3$ in ethanol (Figure 5). All dielectric spectra exhibit the same features. At high frequencies the spectra converge to a constant conductivity σ_∞ and to a real permittivity that corresponds to the dielectric constant of the solvent. At low frequencies, $\epsilon'(\omega)$ increases and $\sigma(\omega)$ decreases due to electrode polarization. In Appendix C, two representative measurements are also plotted in terms of $\epsilon = \epsilon' - i\epsilon''$ and $Z = Z' - iZ''$.

The fits shown in Figures 3−5 were obtained in three steps. First, for each electrolyte, the average diffusion coefficient was calculated from literature data (Table 1). Then for each sample

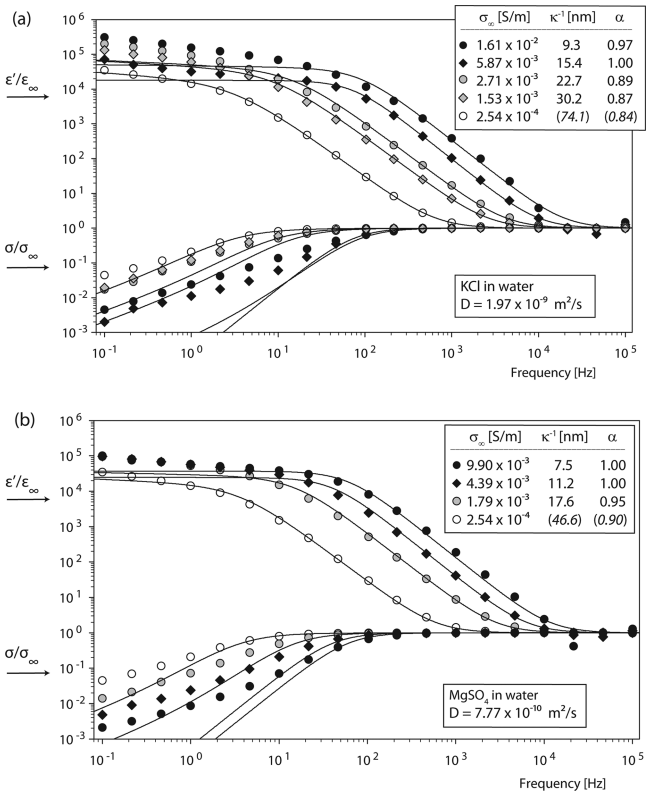

Figure 3. Dielectric spectra of (a) KCl and (b) $MgSO_4$ in water. Symbols denote experimental data at different concentrations; (○) is pure solvent. Solid lines are fits using eq 10 and fit parameters as given in the figure.

the Debye length κ^{-1} was calculated from the conductivity $\sigma_\infty = \epsilon_0\epsilon_s D\kappa^2$. Finally, the value of α in eq 10 was adjusted for an optimal fit in the frequency range above the reciprocal relaxation time τ^{-1}.

The average diffusion coefficients in Table 2 are the average of positive and negative ions $D = (D_+ + D_-)/2$ and were calculated from the data in Table 1. The ionic conductivity in the limit of low salt concentration c_s is $\Lambda^0 = \sigma_\infty/c_s|z|$, with $|z|$ the absolute ion valency. From the Einstein relation $D_i = \mu_i kT/q_i$, the average diffusion coefficient is $D = \sigma_\infty/(\epsilon_0\epsilon_s\kappa^2) = (D_+ + D_-)/2 = kT|z|(\Lambda_+ + \Lambda_-)/(2N_A q^2)$, with N_A the Avogadro constant. Tertbutylammonium and tetraphenylborate ions do not have a solvation shell in organic solvents; hence the Stokes radii a_H are independent of the solvent[31] and the diffusion coefficient is calculated using $D = kT/6\pi\eta a_H$, with η the solvent viscosity. TBATPB in butyl acetate or hexanol does not fully dissociate into free ions, due to the low dielectric constant of the solvents. Instead, many neutral ion pairs are present, which do not contribute to the conductivity. Experimental conductivities of tertbutylammonium salts have been shown to be in good agreement with theory and simulations that describe the equilibrium between free ions and ion pairs.[32] The use of the average diffusion coefficient is justified in Appendix A, where it is shown that the complex permittivity of an asymmetric electrolyte hardly varies for different D_+/D_- ratios while keeping the average diffusion coefficient D constant. Besides the diffusion coefficients, the dielectric constants and electrode spacings are also given in Table 2. Because the empirical model did not exactly match the data over the whole frequency range, data were fitted in the frequency range above the double layer relaxation

dx.doi.org/10.1021/jp5025476 | J. Phys. Chem. C 2014, 118, 11584−11592

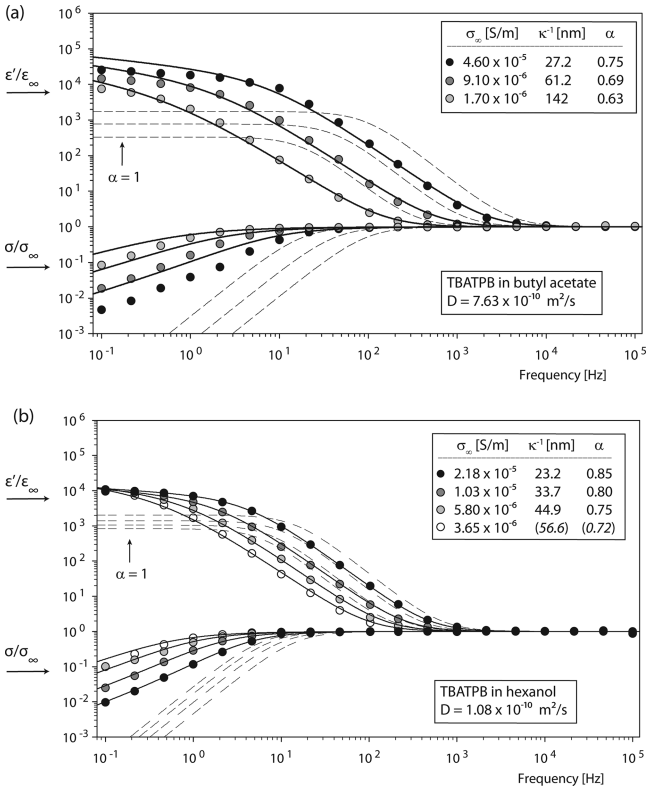

Figure 4. Dielectric spectra of TBATPB in (a) butyl acetate and (b) hexanol. Symbols denote experimental data at different concentrations; (○) is pure solvent. Solid lines are fits using eq 10 and fit parameters as given in the figure. For comparison, spectra for the same parameters are also shown corresponding to $\alpha = 1$.

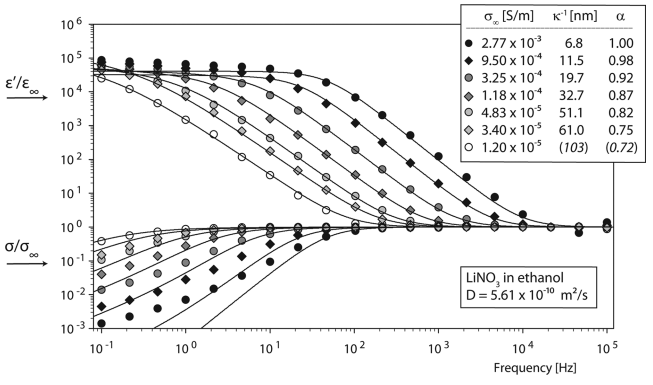

Figure 5. Dielectric spectra of $LiNO_3$ in ethanol. Symbols denote experimental data at different concentrations; (○) is pure solvent. Solid lines are fits using eq 10 and fit parameters as given in the figure.

frequency $\tau^{-1} = 2D\kappa/d$. It was not possible to fit most of the data with the PNP model, for which ϵ' has a slope of −2 (in the region indicated in Figure 1) irrespective of the dielectric constant, diffusion coefficient, or ion density, whereas in most of the data the slope is less negative than −2. The deviation from the PNP model with the data is most dramatic for the TBATPB electrolyte, for which the deviation is indicated in Figure 4. Pure solvents were fitted as well for comparison, but because the diffusion coefficient of the ions still present in these solvents is unknown, these results are omitted in the discussion of our results.

Table 1. Limiting Equivalent Conductivities Λ_0 and Hydrodynamic Radii a_H of the Used Electrolytes As Obtained from the Cited References

electrolyte/solvent	Λ_0 [S cm^2 mol^{-1}]		ref
KCl/water	(K^+)	73.52[a]	33
	(Cl^-)	76.34[a]	33
$MgSO_4$/water	($^1/_2$ Mg^{2+})	47.99[b]	34
	($^1/_2$ SO_4^{2-})	70.47[b]	34
$LiNO_3$/ethanol	($LiNO_3$)	42.74[a]	35
	a_H [Å]		
$(Bu_4N)^+$	3.84		31
$(Ph_4B)^-$	4.08		31

[a]At 25 °C. [b]At 20 °C.

Table 2. Measurement Parameters

electrolyte/solvent	$D = (D_+ + D_-)/2$ [m^2/s]	T [K]	ϵ_s[36]	d [μm]
KCl/water	1.97×10^{-9}	293	80.15	551
$MgSO_4$/water	7.77×10^{-10}	293	80.15	551
$LiNO_3$/ethanol	5.61×10^{-10}	293	25.45	551
TBATPB/hexanol	1.02×10^{-10}	293	12.99	94.6
TBATPB/butyl acetate	7.63×10^{-10}	295	5.04	94.6

5. DISCUSSION

Remarkably, the empirical model based on eq 10 describes the high frequency region of all our data with just one adjustable fit parameter, α. This parameter appears to be strongly dependent on the ionic strength, as illustrated in Figure 6, where α is plotted

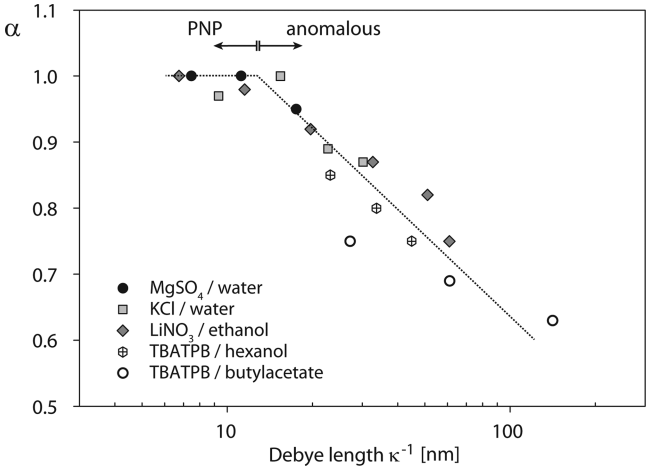

Figure 6. CPE exponent α as a function of Debye length κ^{-1} for dielectric constants from 5 to 80 and ion concentrations from 0.3 μM to 1 mM. The dotted line is a guide to the eye. Below $\kappa^{-1} \approx 10-20$ nm experimental data is in agreement with the Poisson-Nernst−Planck (PNP) model, whereas at larger Debye lengths anomalous behavior is observed with a slope of $c \approx -0.4$ in the following empirical equation: $\alpha = c \cdot \log(\kappa^{-1}[nm]) + 1.44$.

versus the Debye length κ^{-1}. Aqueous and ethanolic solutions at concentrations above 0.25 mM are well fitted with $\alpha = 1$; hence they show the expected response of the PNP model (eq 5). This is in agreement with other reports of measurements at similar ionic strengths using a parallel plate capacitor[37,38] or cylindrical capacitor.[39] Decreasing ionic strength leads to a decrease of α, down to $\alpha = 0.6-0.7$ for the lowest ionic strengths. Above $\kappa^{-1} \approx 10-20$ nm, α decreases with a slope of $c = -0.4$ in the empirical

dx.doi.org/10.1021/jp5025476 | J. Phys. Chem. C 2014, 118, 11584−11592

relation $\alpha = c{\cdot}\log(\kappa^{-1}[nm]) + 1.44$. Others find at even lower ionic strength in apolar solvents an $\omega^{-3/2}$ frequency dependence of $\epsilon'(\omega)$,[40−44] corresponding to $\alpha = 0.5$, which is consistent with our observations as well. A quantitative relation to physical parameters, however, was not given in these studies, and the observed frequency dependence was incorrectly ascribed to the PNP model, as explained by Hollingsworth.[24]

At lower frequencies, below the double layer relaxation frequency τ^{-1}, the agreement of the model with the data varies per measurement. Nevertheless, the model captures the general trend, especially for the lowest ionic strengths. In this frequency range, double layers are strongly charged due to an increased counterion concentration at the electrodes, amplifying the electric field at the electrodes by a factor of $|\epsilon'(\omega)/\epsilon_\infty| \approx 10^4-10^5$ compared to the electric field without electrode polarization, $E_0 = V_0/d$, with V_0 the applied potential. Possible nonidealities at the lowest frequencies related to the increased electric field and ion concentrations near the electrodes, ion absorption, or association/dissociation of ion pairs are beyond the scope of this paper; in principle, such effects might be modeled as an addition to the PNP equations. Here, we will argue that the high frequency double layer behavior is not related to any of these effects; instead, it is related to a failure of the PNP equations themselves. To prevent low frequency effects from complicating the analysis, we focus on the higher frequency range above $\tau^{-1} = 2D\kappa/d$, where the double layer is not yet fully charged.

In finding a rationale for the ionic strength dependence of α and the specific form of the CPE, a first important point to be noticed is that deviations from the PNP model start already at high frequencies when $\epsilon'/\epsilon_\infty < 10$. In this situation the electric field in the capacitor is still relatively homogeneous, and the variation in ion concentrations is small. Therefore, no effect of ion association or dissociation on the response[20] is expected; this is further illustrated in Appendix B. In our experiments there is no large difference in the behavior of the strongly associated TBATPB and strongly dissociated electrolytes (KCl, $MgSO_4$, $LiNO_3$), except for the continuing trend of decreasing α with decreasing ionic strength. The rate of electrolyte dissociation is expected to increase above an electric field strength of 10^6-10^7 V/m,[45] but this occurs at much higher field strengths than the field $V_0/d \approx 250$ V/m applied here. It should be kept in mind, however, that the field near the electrodes is strongly amplified; hence the dissociation rate might increase at low frequencies, when the electrodes are strongly polarized. A second point to notice is that the apparent double layer formation is slower than expected, rather than being faster. This excludes the absorption of ions onto the electrodes as major cause of capacitance dispersion. Adsorption of ions onto the electrodes will lead to an additional increase of the permittivity,[46] which might occur at low frequency. It will, however, not lead to a slower double layer formation, but it will accelerate the process.

It has been suggested that capacitance dispersion is caused by electrode roughness and that the CPE exponent is related to the fractal dimension of the rough electrode surface.[47−49] Experiments, however, suggest that there is no correlation between electrode roughness and the CPE exponent.[50,51] Furthermore, thin double layers are expected to follow the surface curvature better than thick double layers; thus they are expected to show a stronger effect of surface roughness, contrary to our observation of $\alpha < 1$ for thick double layers. Alternatively, it has been suggested that capacitance dispersion might be caused by physicochemical heterogeneities on the electrode surface.[51−53]

We measured the response of both strongly dissociated and associated electrolytes, both monovalent and divalent ions, and solvents of different dielectric constants. The trend in the dependence of α on κ^{-1} (Figure 6) suggests that the underlying cause is not specific for one particular system, but general. At low ionic strength, for a double layer thickness $\kappa^{-1} > 10-20$ nm, double layer dynamics become markedly different. The electrolyte circuit of the empirical model (Figure 2c) has the double layer capacitance replaced by a CPE element. Apart from the double layer relaxation no other frequency dispersion is observed, and $\epsilon'(\omega)$ and $\sigma(\omega)$ are constant at frequencies above the electrode polarization. Thus, it appears that deviations from the PNP equations occur in the double layer, rather than in the bulk of the electrolyte solution.

The PNP equations describe transport of ions without an effect of interactions between ions, except in an average way via the macroscopic electric field computed by the Poisson equation. Decreasing the ionic strength would only increase the average distance between the ions, and therefore an effect of the magnitude of the ion interactions is not be expected. At lower ionic strength, however, the range of interaction does increase. The Coulomb interaction potential in ionic solutions is screened by an ionic cloud and effectively short-range ($U(r) \propto e^{-\kappa r}/r$), but within a Debye length κ^{-1} the potential decays slowly with distance ($U(r) \propto 1/r$). As the ionic strength decreases, the average number N_D of ions within a Debye sphere increases as $N_D = (4/3)\pi n(\kappa^{-1})^3 \propto n^{-1/2}$. The obtained result here poses a question about the use of Fick's law of diffusion, at least valid for noninteracting particles, for describing the collective dynamics of interacting ions. The double layer dynamics, here relaxation toward equilibrium in the presence of an external field, are influenced at low ionic strength by the long-range nature of the Coulombic interaction. Effects of the long-range Coulomb interaction become apparent in nonequilibrium plasmas, where non-Maxwellian or power-law electron velocity distributions have been observed.[54−56] Double layers are also crucial in dispersions of charged colloids, in which unexplained observations at low ionic strength have been made.[57−59]

Transport properties have also been discussed in terms of anomalous diffusion, by varying the time dependence of the mean square displacement.[60] Frequency responses of an electrolyte with the assumption of anomalous diffusion have been calculated recently[61,62] (by which also the time dependence of drift was modified via the Einstein relation), but these could not describe our data in a consistent way. Modification of the PNP equations, perhaps by adjusting Fick's law (first term of right-hand side of eq 1), might yield transport equations that describe our data. Although the empirical model describing our data is specific for the geometry of the parallel plate capacitor, the modified PNP equations could be tested for different geometries as well.

Although we have focused on the frequency domain, similar measurements have been performed in the time domain, where the current of charged micelles in apolar solvents was measured after the application of a step voltage.[63,64] Apart from exponentially decaying current, also power law behavior was observed.[63] We evaluated the time response of the equivalent circuit in Figure 2c (derivation in Appendix D) and, for $\alpha < 1$, observe power law behavior as well. The CPE response of the double layer is likely to apply as well to these measurements in the time domain.

6. CONCLUSIONS

For moderate to high salt concentrations (≥0.25 mM), the frequency dependence of electrode polarization at frequencies above the double layer relaxation frequency is in excellent agreement with the Poisson−Nernst−Planck (PNP) model that accounts for diffusion and drift without ion interactions. At lower ionic strength, however, the measurements deviate from this model and exhibit capacitance dispersion. We find empirically that the anomalous response of the double layer capacitance C_{dl} can be described well as a CPE with impedance $Z^{-1} = (C_{dl}/\tau_\infty)(i\omega\tau_\infty)^\alpha$. Our experiments highlight the influence of the ionic strength on the frequency dispersion of electrode polarization through the parameter α. Double layer dynamics become markedly different above a Debye length of 10−20 nm, which is possibly related to the long-range nature of the Coulomb interaction.

APPENDIX A: ASYMMETRIC ELECTROLYTE

The response of an asymmetric electrolyte, with unequal diffusion coefficients $D_+ \neq D_-$, was also considered in the work of Macdonald.[20] Analogous to the derivation of the symmetric PNP model, but with $D_+ \neq D_-$, though $q_+ = q_-$ and the Einstein relation still applies, the complex permittivity is given by

$$\frac{\epsilon(\omega)}{\epsilon_s} = \left[\lambda_+ \cosh\left(\frac{\lambda_+ d}{2}\right) + \chi\lambda_- \cosh\left(\frac{\lambda_- d}{2}\right)\right] \Big/ \left[\left(\chi\lambda_- - \frac{\kappa^2}{2}\frac{\chi(1-\gamma^-)}{\lambda_-}\right)\cosh\left(\frac{\lambda_- d}{2}\right) + \left(\lambda_+ - \frac{\kappa^2}{2}\frac{1-\gamma^+}{\lambda_+}\right)\cosh\left(\frac{\lambda_+ d}{2}\right) + \frac{\kappa^2}{d}\left(\frac{1-\gamma^+}{{\lambda_+}^2}\sinh\left(\frac{\lambda_+ d}{2}\right) + \frac{\chi(1-\gamma^-)}{{\lambda_-}^2}\sinh\left(\frac{\lambda_- d}{2}\right)\right)\right] \tag{11}$$

with

$${\lambda_\pm}^2 = \frac{1}{2}\left(\kappa^2 + \frac{i\omega}{D_+} + \frac{i\omega}{D_-}\right) \pm \frac{1}{2}\sqrt{\kappa^4 - \left(\frac{\omega}{D_+} - \frac{\omega}{D_-}\right)^2} \tag{12}$$

$$\gamma^\pm = -\frac{2}{\kappa^2}\left({\lambda_\pm}^2 - \kappa^2/2 - i\frac{\omega}{D_+}\right) \tag{13}$$

$$\chi = \frac{-\lambda_+(1+\gamma^+)\cosh(\lambda_+ d/2)}{\lambda_-(1+\gamma^-)\cosh(\lambda_- d/2)} \tag{14}$$

This function for an asymmetric electrolyte is plotted in Figure 7 for three different D_+/D_- ratios, while keeping the average diffusion coefficient D, and hence the conductivity σ_∞, constant. The response hardly depends on the D_+/D_- ratio. Therefore, it seems justified to use the average diffusion coefficient in the empirical model, eq 10. For comparison, the value of the average diffusion coefficient, rather than the ratio, has a much stronger influence on the response, as is shown in Figure 8.

APPENDIX B: ASSOCIATION/DISSOCIATION

Positive and negative ions might form neutral ion pairs, which do not contribute to the conductivity or double layer, especially in solvents with a low dielectric constant. The influence of association or dissociation of charge carriers has also been modeled by Macdonald;[20] however, its influence on the response in the frequency range above the double layer relaxation time is very small. The equilibrium between positive and negative ions, with concentrations n_+ and n_-, and neutral ion pairs, with concentration n_0, could be described by an equilibrium constant $K = n_+ n_- / {n_0}^2$.

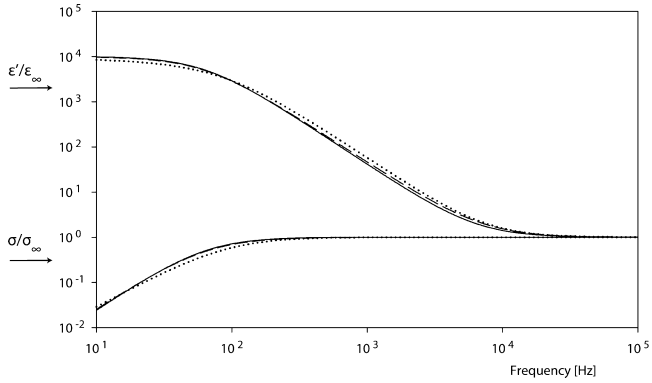

Figure 7. Response of an asymmetric electrolyte (using eq 11) for three different diffusion coefficient ratios: $D_+/D_- = 1$ (solid line), $D_+/D_- = 10^{-2}$ (dashed line), $D_+/D_- = 10^{-4}$ (dotted line) with the same average diffusion coefficient $D = (D_+ + D_-)/2 = 10^{-10}$ m^2 s^{-1}, $\kappa^{-1} = 5$ nm, and $d = 100$ μm.

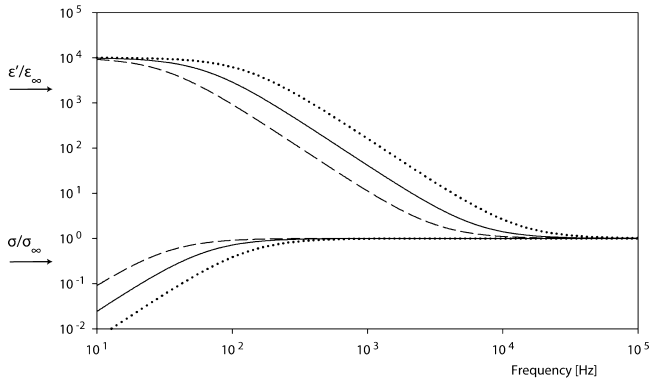

Figure 8. Response of a symmetric electrolyte (using eq 5) for $D = 1 \times 10^{-10}$ m^2 s^{-1} (solid line), $D = 0.5 \times 10^{-10}$ m^2 s^{-1} (dashed line), $D = 2 \times 10^{-10}$ m^2 s^{-1} (dotted line), with $\kappa^{-1} = 5$ nm, and $d = 100$ μm.

The deviation of the ion concentrations relative to the average ion concentration, $\eta_\pm/n$, without association or dissociation, is given by[22]

$$\left|\frac{\eta_\pm(z)}{n_0}\right| = \left|\frac{(q\lambda/2kT)\sinh(\lambda z)}{(\kappa^2/\lambda)\sinh(\lambda d/2) + i(\omega d/2D)\cosh(\lambda d/2)}V_0\right| \tag{15}$$

According to the PNP model without association or dissociation (eq 10 and eq 15), the (absolute) product $n_+(z)$ $n_-(z) = (n + \eta_+(z))(n + \eta_-(z)) = n^2 - {\eta_+}^2(z)$ is the largest near the electrodes at $z = \pm d/2$. At the double layer relaxation frequency τ^{-1} this product $n_+(z)$ $n_-(z) = 0.88$ n^2 is close to the product of the average concentrations for typical values of $D = 10^{-9}$ m^2/s, $\kappa^{-1} = 10$ nm, $V_0 = 25$ mV, and $d = 100$ μm. At a frequency higher by a factor of 10, the product $n_+(d/2)$ $n_-(d/2)$ $= 0.998$ $n^2 \approx n^2$ becomes almost spatially and frequency independent and a shift in the equilibrium is not expected.

APPENDIX C: ADDITIONAL PLOTS

Instead of $\epsilon'/\epsilon_\infty$ and σ/σ_∞, dielectric spectra could also be expressed in terms of the complex permittivity $\epsilon = \epsilon' - i\epsilon''$ or the impedance $Z = Z' - iZ''$. Figure 9 shows such alternatives for two measurements of $LiNO_3$ in ethanol.

dx.doi.org/10.1021/jp5025476 | J. Phys. Chem. C 2014, 118, 11584−11592

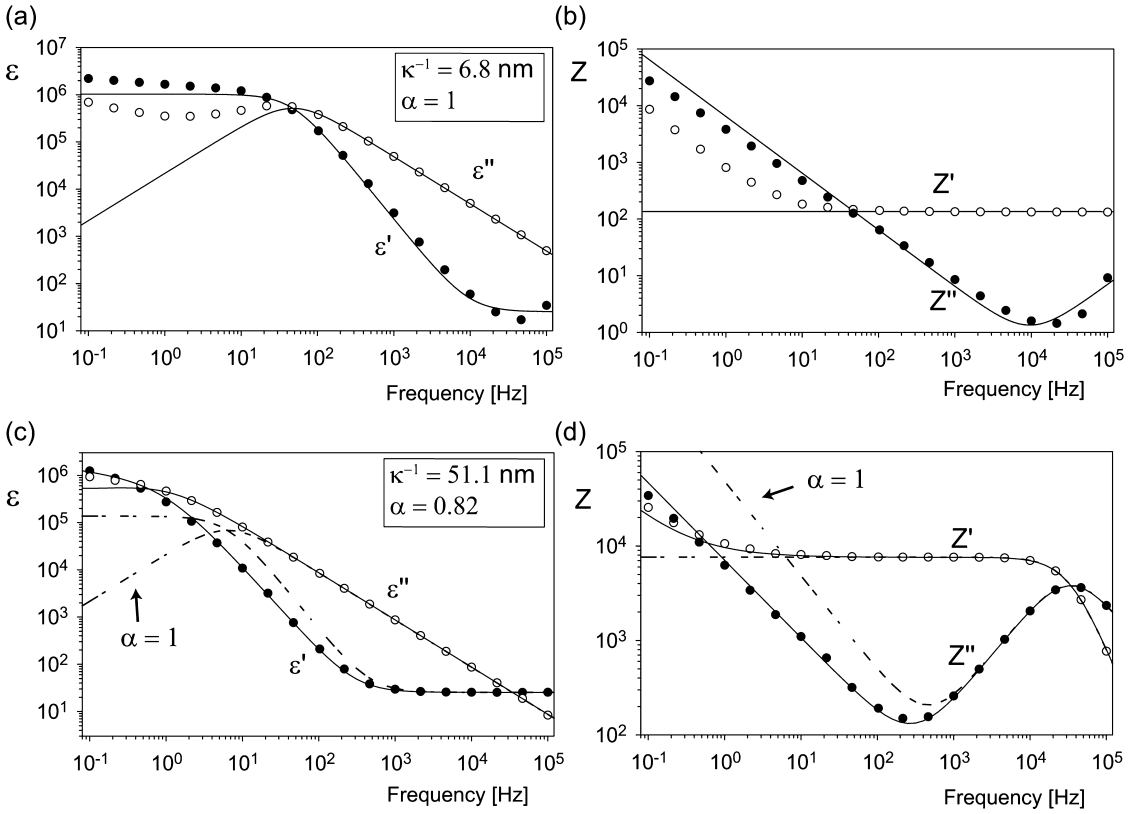

Figure 9. Additional plots for two measurements on $LiNO_3$ in ethanol, in terms of $\epsilon = \epsilon' - i\epsilon''$ (a,c) and $Z[\Omega] = Z' - iZ''$ (b,d). Original data is plotted in Figure 5.

APPENDIX D: TIME RESPONSE

The response of the equivalent circuit in Figure 2c, which corresponds well with our experimental data, is evaluated in the time domain, with the use of the Laplace transform, defined by $\mathcal{L}\{f(t)\} \equiv \int_0^\infty e^{-st} f(t)\, dt = F(s)$. The current $i(t)$, with Laplace transform $\mathcal{L}\{i(t)\} = I(s)$, is calculated when a step input voltage $v(t) = V_0$ for $t \geq 0$ is applied, with Laplace transform $\mathcal{L}\{v(t)\} = V(s) = V_0/s$. The impedance $Z(s) = V(s)/I(s)$ of the resistor in series with the CPE element is given by

$$Z(s) = R + \left(\frac{\tau^{1-\alpha}}{C_{dl}}\right) s^{-\alpha} \tag{16}$$

Then, the current $i(t)$ is

$$i(t) = \mathcal{L}^{-1}\left\{\frac{V(s)}{Z(s)}\right\} = \mathcal{L}^{-1}\left\{\frac{V_0/s}{R + (\tau^{1-\alpha}/C_{dl})s^{-\alpha}}\right\}$$
$$= \frac{V_0}{R}\cdot\mathcal{L}^{-1}\left\{\frac{1}{s}\cdot\frac{s^\alpha}{s^\alpha + \tau_\infty^{1-\alpha}/RC_{dl}}\right\} \tag{17}$$

To solve the inverse Laplace transform $\mathcal{L}^{-1}$, the following Laplace transform is used:[65]

$$\mathcal{L}\{E_{\alpha,1}[-at^\alpha]\} = \frac{1}{s}\left(\frac{s^\alpha}{s^\alpha + a}\right) \tag{18}$$

where the generalized Mittag–Leffner function is given by

$$E_{\alpha,\beta}[x] = \sum_{k=0}^{\infty} \frac{x^k}{\Gamma(\alpha k + \beta)} \tag{19}$$

where α and β are positive real constants and Γ is the gamma function. A special case of the Mittag–Leffner function is $E_{1,1}[x] = \sum_{k=0}^{\infty} x^k/k! = e^x$. The current is obtained by using eq 18 and substitution of the double layer relaxation time $\tau = RC_{dl}$:

$$i(t) = \frac{V_0}{R} E_{\alpha,1}[-(\tau_\infty^{1-\alpha}/\tau)t^\alpha] = \frac{V_0}{R}\sum_{k=0}^{\infty}\frac{(-\tau_\infty^{1-\alpha}/\tau)^k t^{\alpha k}}{\Gamma(\alpha k + 1)} \tag{20}$$

For $\alpha = 1$, the CPE element reduces to an ideal capacitor, and the current decays exponentially:

$$i(t) = \frac{V_0}{R}\sum_{k=0}^{\infty}\frac{(-t/\tau)^k}{k!} = \frac{V_0}{R} e^{-t/\tau} \tag{21}$$

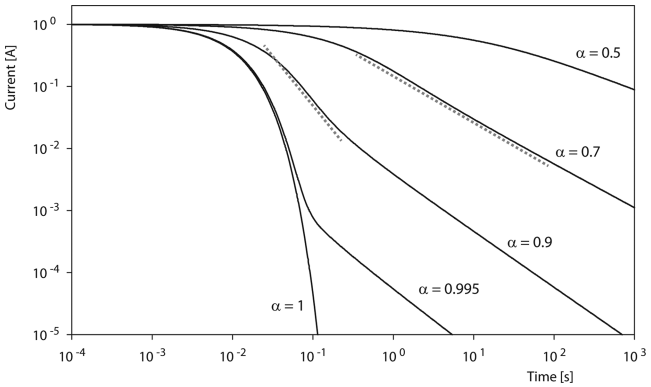

Figure 10. Time response of the equivalent circuit in Figure 2c. The current $i(t)$ is shown as a function of time t after application of a step voltage, calculated for different values of α, with $\tau = 10^{-2}$ s, $\tau_\infty = 4 \times 10^{-6}$ s, and normalized with $V_0/R = 1$ A. Power law behavior is indicated by the dashed lines.

dx.doi.org/10.1021/jp5025476 | J. Phys. Chem. C 2014, 118, 11584–11592

The response is evaluated[66] for a few values of α in Figure 10. For lower values of α, the formation of the double layer is slower, equivalent to the frequency domain.

AUTHOR INFORMATION

Corresponding Author

*B. Erné: e-mail, b.h.erne@uu.nl.

Notes

The authors declare no competing financial interest.

ACKNOWLEDGMENTS

We acknowledge Andrew Hollingsworth, René van Roij, Andrei Petukhov, Jan Groenewold, Alwin Verschueren, and Casper van der Wel for useful discussions. This work was supported by The Netherlands Organisation for Scientific Research (NWO).

REFERENCES

(1) Schwan, H. P. Electrode Polarization Impedance and Measurements in Biological Materials. *Ann. N. Y. Acad. Sci.* **1968**, *148*, 191.

(2) Dyre, J. C.; Maass, P.; Roling, B.; Sidebottom, D. L. Fundamental Questions Relating to Ion Conduction in Disordered Solids. *Rep. Prog. Phys.* **2009**, *72*, 046501.

(3) Springer, M. M.; Korteweg, A.; Lyklema, J. The Relaxation of the Double-Layer around Colloid Particles and the Low-Frequency Dielectric-Dispersion: Part II. Experiments. *J. Electroanal. Chem.* **1983**, *153*, 55−66.

(4) Winter, M.; Brodd, R. J. What are Batteries, Fuel Cells, and Supercapacitors? *Chem. Rev.* **2004**, *104*, 4245−4269.

(5) Comiskey, B.; Albert, J. D.; Yoshizawa, H.; Jacobson, J. An Electrophoretic Ink for All-Printed Reflective Electronic Displays. *Nature* **1998**, *394*, 253−255.

(6) Minerick, A. R.; Zhou, R. H.; Takhistov, P.; Chang, H. C. Manipulation and Characterization of Red Blood Cells with Alternating Current Fields in Microdevices. *Electrophoresis* **2003**, *24*, 3703−3717.

(7) Wolff, I. A Study of Polarization Capacity over a Wide Frequency Band. *Phys. Rev.* **1926**, *27*, 755−763.

(8) Fricke, R. The Theory of Electrolytic Polarization. *Philos. Mag.* **1932**, *14*, 310−318.

(9) Scheider, W. Theory of Frequency Dispersion of Electrode Polarization - Topology of Networks with Fractional Power Frequency-Dependence. *J. Phys. Chem.* **1975**, *79*, 127−136.

(10) Brug, G. J.; van den Eeden, A. L. G.; Sluyters-Rehbach, M.; Sluyters, J. H. The Analysis of Electrode Impedances Complicated by the Presence of a Constant Phase Element. *J. Electroanal. Chem.* **1984**, *176*, 275−295.

(11) Cole, K. S.; Cole, R. H. Dispersion and Absorption in Dielectrics I. Alternating Current Characteristics. *J. Chem. Phys.* **1941**, *9*, 341−351.

(12) Jonscher, A. K. A New Understanding of the Dielectric-Relaxation of Solids. *J. Mater. Sci.* **1981**, *16*, 2037−2060.

(13) Macdonald, J. R. Note on the Parameterization of the Constant-Phase Admittance Element. *Solid State Ionics* **1984**, *13*, 147−149.

(14) Zoltowski, P. On the Electrical Capacitance of Interfaces Exhibiting Constant Phase Element Behaviour. *J. Electroanal. Chem.* **1998**, *443*, 149−154.

(15) Lang, G.; Heusler, K. E. Remarks on the Energetics of Interfaces Exhibiting Constant Phase Element Behaviour. *J. Electroanal. Chem.* **1998**, *457*, 257−260.

(16) Sadkowski, A. On the Ideal Polarisability of Electrodes Displaying CPE-type Capacitance Dispersion. *J. Electroanal. Chem.* **2000**, *481*, 222−226.

(17) Lang, G.; Heusler, K. E. Comments on the Ideal Polarisability of Electrodes Displaying CPE-type Capacitance Dispersion. *J. Electroanal. Chem.* **2000**, *481*, 227−229.

(18) Zoltowski, P. Comments on the Paper 'On the Ideal Polarisability of Electrodes Displaying CPE-type Capacitance Dispersion' by A. Sadkowski. *J. Electroanal. Chem.* **2000**, *481*, 230−231.

(19) Sadkowski, A. Response to the 'Comments on the Ideal Polarisability of Electrodes Displaying CPE-type Capacitance Dispersion' by G. Lang, K.E. Heusler. *J. Electroanal. Chem.* **2000**, *481*, 232−236.

(20) Macdonald, J. R. Theory of AC Space-Charge Polarization Effects in Photoconductors, Semiconductors, and Electrolytes. *Phys. Rev.* **1953**, *92*, 4−17.

(21) Macdonald, J. R. Utility of Continuum Diffusion Models for Analyzing Mobile-Ion Immittance Data: Electrode Polarization, Bulk, and Generation-Recombination Effects. *J. Phys.: Condens. Matter* **2010**, *22*, 495101.

(22) Barbero, G.; Alexe-Ionescu, A. L. Role of the Diffuse Layer of the Ionic Charge on the Impedance Spectroscopy of a Cell of Liquid. *Liq. Cryst.* **2005**, *32*, 943−949.

(23) Macdonald, J. R. Electrical Response of Materials Containing Space Charge with Discharge at Electrodes. *J. Chem. Phys.* **1971**, *54*, 2026−2050.

(24) Hollingsworth, A. D. Remarks on the Determination of Low-Frequency Measurements of the Dielectric Response of Colloidal Suspensions. *Curr. Opin. Colloid Interface Sci.* **2013**, *18*, 157−159.

(25) Coelho, R. On the Relaxation of a Space-Charge. *Rev. Phys. Appl.* **1983**, *18*, 137−146.

(26) Coelho, R. On the Static Permittivity of Dipolar and Conductive Media - an Educational-Approach. *J. Non-Cryst. Solids* **1991**, *131*, 1136−1139.

(27) Klein, R. J.; Zhang, S.; Dou, S.; Jones, B. H.; Colby, R. H.; Runt, J. Modeling Electrode Polarization in Dielectric Spectroscopy: Ion Mobility and Mobile Ion Concentration of Single-Ion Polymer Electrolytes. *J. Chem. Phys.* **2006**, *124*, 144903.

(28) The approximation is valid for $\kappa^{-1} \ll d$ (and therefore $\Delta\epsilon/\epsilon_s \gg 1$). When $\omega \ll \tau_\infty^{-1}$, then $\lambda d/2 = \Delta\epsilon/\epsilon_s$ and $\tanh(\lambda d/2) = 1$; the exact solution rewritten as $\epsilon(\omega) = \epsilon_s[1 + (\lambda d/2 - 1)/(1 + i\omega\tau_\infty\lambda d/2)]$ reduces to the Debye relaxation (eq 7). When ω is not $\ll \tau_\infty^{-1}$, then $\omega \gg \tau^{-1}$ (because $\tau = \tau_\infty\Delta\epsilon/\epsilon_s \gg \tau_\infty$) and $\tanh(\lambda d/2) = (\exp(\lambda d) - 1)/(\exp(\lambda d) + 1) \approx 1$; the exact solution $\epsilon(\omega) = (1 + i\omega\tau_\infty)\epsilon_s\lambda d/2/[\tanh(\lambda d/2) + i\omega\tau_\infty\lambda d/2]$ reduces to $\epsilon(\omega) \approx \epsilon_s + i\Delta\epsilon/\omega\tau$ with the real part equal to the solvent dielectric constant and the imaginary part representing the conductivity ($\sigma = \epsilon_0\epsilon_s D\kappa^2 = \omega\epsilon_0\epsilon''$), which is also what the Debye relaxation reduces to for $\omega \gg \tau^{-1}$. Thus, the effect of electrode polarization is not well described only for $\omega \gg \tau_\infty^{-1}$, when this effect itself is much smaller than that of the solvent. The Debye relaxation is a good approximation over the whole frequency range under the condition $\kappa^{-1} \ll d$.

(29) Macdonald, J. R.; Evangelista, L. R.; Lenzi, E. K.; Barbero, G. Comparison of Impedance Spectroscopy Expressions and Responses of Alternate Anomalous Poisson-Nernst-Planck Diffusion Equations for Finite-Length Situations. *J. Phys. Chem. C* **2011**, *115*, 7648−7655.

(30) Kortschot, R. J.; Bakelaar, I. A.; Erné, B. H.; Kuipers, B. W. M. A Differential Dielectric Spectroscopy Setup to Measure the Electric Dipole Moment and Net Charge of Colloidal Quantum Dots. *Rev. Sci. Instrum.* **2014**, *85*, 033903.

(31) Krumgalz, B. S. Dimensions of Tetra-alkyl(aryl)onium Ions. *J. Chem. Soc., Faraday Trans. I* **1982**, *78*, 437−449.

(32) Valeriani, C.; Camp, P. J.; Zwanikken, J. W.; van Roij, R.; Dijkstra, M. Ion Association in Low-Polarity Solvents: Comparisons between Theory, Simulation, and Experiment. *Soft Matter* **2010**, *6*, 2793−2800.

(33) Harned, H. S.; Owen, B. B. *The Physical Chemistry of Electrolyte Solutions*; Reinhold Publishing Corp.: New York, 1950; p 172.

(34) Tomsic, M.; Bester-Rogac, M.; Jamnik, A.; Neueder, R.; Barthel, J. Conductivity of Magnesium Sulfate in Water from 5 to 35 Degrees C and from Infinite Dilution to Saturation. *J. Solution Chem.* **2002**, *31*, 19−31.

(35) Parfitt, G. D.; Smith, A. L. Conductance of Silver, Potassium and Lithium Nitrates in Ethanol-Water Mixtures. *Trans. Faraday Soc.* **1963**, *59*, 257.

(36) Permittivity (Dielectric Constant) of Liquids. *CRC Handbook of Chemistry and Physics*, 93rd ed.; CRC Press: Boca Raton, FL, 2012; http://www.hbcpnetbase.com, accessed 2012.

(37) Chassagne, C.; Bedeaux, D.; van der Ploeg, J. P. M.; Koper, G. J. M. Theory of Electrode Polarization: Application to Parallel Plate Cell Dielectric Spectroscopy Experiments. *Colloid Interfaces A* **2002**, *210*, 137−145.
(38) Hollingsworth, A. D.; Saville, D. A. A Broad Frequency Range Dielectric Spectrometer for Colloidal Suspensions: Cell Design, Calibration, and Validation. *J. Colloid Interface Sci.* **2003**, *257*, 65−76.
(39) Chassagne, C.; Bedeaux, D.; van der Ploeg, J. P. M.; Koper, G. J. M. Polarization between Concentric Cylindrical Electrodes. *Physica A* **2003**, *326*, 129−140.
(40) Uemura, S. Low-Frequency Dielectric Behavior of Poly-(vinylidene fluoride). *J. Polym. Sci., Part B: Polym. Phys.* **1974**, *12*, 1177−1188.
(41) Murakami, S.; Iga, H.; Naito, H. Dielectric Properties of Nematic Liquid Crystals in the Ultralow Frequency Regime. *J. Appl. Phys.* **1996**, *80*, 6396−6400.
(42) Cirkel, P. A.; van der Ploeg, J. P. M.; Koper, G. J. M. Electrode Effects in Dielectric Spectroscopy of Colloidal Suspensions. *Physica A* **1997**, *235*, 269−278.
(43) Shim, M.; Guyot-Sionnest, P. Permanent Dipole Moment and Charges in Colloidal Semiconductor Quantum Dots. *J. Chem. Phys.* **1999**, *111*, 6955−6964.
(44) Sawada, A. Internal Electric Fields of Electrolytic Solutions Induced by Space-Charge Polarization. *J. Appl. Phys.* **2006**, *100*, 074103.
(45) Onsager, L. Deviations from Ohm's Law in Weak Electrolytes. *J. Chem. Phys.* **1934**, *2*, 599−615.
(46) Barbero, G. Influence of Adsorption Phenomenon on the Impedance Spectroscopy of a Cell of Liquid. *Phys. Rev. E* **2005**, *71*, 062201.
(47) de Levie, R. The Influence of Surface Roughness of Solid Electrodes on Electrochemical Measurements. *Electrochim. Acta* **1965**, *10*, 113−130.
(48) Le Mehaute, A.; Crepy, G. Introduction to Transfer and Motion in Fractal Media - the Geometry of Kinetics. *Solid State Ionics* **1983**, *9*−*10*, 17−30.
(49) Nyikos, L.; Pajkossy, T. Fractal Dimension and Fractional Power Frequency- Dependent Impedance of Blocking Electrodes. *Electrochim. Acta* **1985**, *30*, 1533−1540.
(50) Bates, J. B.; Chu, Y. T.; Stribling, W. T. Surface-Topography and Impedance of Metal- Electrolyte Interfaces. *Phys. Rev. Lett.* **1988**, *60*, 627−630.
(51) Pajkossy, T. Impedance of Rough Capacitive Electrodes. *J. Electroanal. Chem.* **1994**, *364*, 111−125.
(52) Kerner, Z.; Pajkossy, T. Impedance of Rough Capacitive Electrodes: the Role of Surface Disorder. *J. Electroanal. Chem.* **1998**, *448*, 139−142.
(53) Pajkossy, T. Impedance Spectroscopy at Interfaces of Metals and Aqueous Solutions - Surface Roughness, CPE and Related Issues. *Solid State Ionics* **2005**, *176*, 1997−2003.
(54) Liu, J. M.; de Groot, J. S.; Matte, J. P.; Johnston, T. W.; Drake, R. P. Measurements of Inverse Bremsstrahlung Absorption and Non-Maxwellian Electron Velocity Distributions. *Phys. Rev. Lett.* **1994**, *72*, 2717−2720.
(55) Lima, J. A. S.; Silva, R.; Santos, J. Plasma Oscillations and Nonextensive Statistics. *Phys. Rev. E* **2000**, *61*, 3260−3263.
(56) Du, J. L. Nonextensivity in Nonequilibrium Plasma Systems with Coulombian Long- Range Interactions. *Phys. Lett. A* **2004**, *329*, 262−267.
(57) Ito, K.; Yoshida, H.; Ise, N. Void Structure in Colloidal Dispersions. *Science* **1994**, *263*, 66−68.
(58) Larsen, A. E.; Grier, D. G. Like-Charge Attractions in Metastable Colloidal Crystallites. *Nature* **1997**, *385*, 230−233.
(59) Philipse, A. P.; Koenderink, G. H. Sedimentation-Diffusion Profiles and Layered Sedimentation of Charged Colloids at Low Ionic Strength. *Adv. Colloid Interface Sci.* **2003**, *100*, 613−639.
(60) Metzler, R.; Klafter, J. The Random Walk's Guide to Anomalous Diffusion: a Fractional Dynamics Approach. *Phys. Rep.* **2000**, *339*, 1−77.
(61) Lenzi, E. K.; Evangelista, L. R.; Barbero, G. Fractional Diffusion Equation and Impedance Spectroscopy of Electrolytic Cells. *J. Phys. Chem. B* **2009**, *113*, 11371−11374.
(62) Evangelista, L. R.; Lenzi, E. K.; Barbero, G.; Macdonald, J. R. Anomalous Diffusion and Memory Effects on the Impedance Spectroscopy for Finite-Length Situations. *J. Phys.: Condens. Matter* **2011**, *23*, 485005.
(63) Beunis, F.; Strubbe, F.; Neyts, K.; Verschueren, A. R. M. Power-Law Transient Charge Transport in a Nonpolar Liquid. *Appl. Phys. Lett.* **2007**, *90*, 182103.
(64) Beunis, F.; Strubbe, F.; Marescaux, M.; Beeckman, J.; Neyts, K.; Verschueren, A. R. M. Dynamics of Charge Transport in Planar Devices. *Phys. Rev. E* **2008**, *78*, 011502.
(65) Das, S. *Functional Fractional Calculus*; Springer-Verlag: Berlin, 2011; eBook pp 351−353.
(66) The Mittag−Leffner function converges, and it was evaluated using the implemented function in Wolfram Mathematica 9.0.